2009 American Control Conference
Hyatt Regency Riverfront, St. Louis, MO, USA
June 10-12, 2009

Experimental results on LPV stabilization of a riderless bicycle

D. Andreo, V. Cerone, D. Dzung, D. Regruto

Abstract— **In this paper the problem of designing a control system aiming at automatically balancing a riderless bicycle in the upright position is considered. Such a problem is formulated as the design of a linear-parameter-varying (LPV) state-feedback controller which guarantees stability of the bicycle when the velocity ranges in a given interval and its derivative is bounded. The designed control system has been implemented on a real riderless bicycle equipped with suitable sensors and actuators, exploiting the processing platform ABB PEC80. The obtained experimental results showed the effectiveness of the proposed approach.**

Index Terms— **Bicycle Dynamics, LPV control.**

I. Introduction

Modeling, analysis and control of bicycle dynamics has been an attractive area of research since the end of the 19th century. Pioneering works on bicycle mathematical modeling were presented in papers [1], [2] and [3]. Rankine in [1] presents a qualitative analysis of both roll and steer dynamics of a bicycle. A quantitative stability analysis was independently developed by Whipple [2] and Carvallo [3] which derived equations of motion linearized around the upright vertical equilibrium. The obtained model was used to formally show that bicycles can balance themselves when running in a proper speed range (self-stability property). Although papers on bicycle modeling regularly appeared also during the first half of the 20th century (see, e.g., the extensive literature reviews presented in [4] and [5]), bicycle dynamics has received a significantly renewed attention since 1970 mainly due to the fast improvement of computers performance and the development of effective software packages for the simulations of complex mathematical models. Computer simulations of a nonlinear bicycle model were presented in the paper by Roland [6]. A good deal of remarkable works about modeling and analysis of bicycle dynamics have been recently conducted by Schwab and coworkers at Delft Bicycle Dynamics Lab (see [7], [8], [9] and the references therein). More specifically they provide a benchmark linearized model of the bicycle dynamics on the basis of the results derived from the comparison between the original model proposed by Whipple and numerical linearization of nonlinear models obtained exploiting different softwares for multibody systems modeling. Recently bicycle dynamics attracted the attention of the automatic control research community. Since bicycle dynamics strongly depends on the forward velocity and, under certain conditions, it can show both right half plane poles and zeros (see, e.g., [4]), the design of feedback controllers for either balancing the bicycle in the upright position (stabilization) or moving the bicycle along a predefined path (trajectory tracking) is indeed a challenging problem. A deep analysis of the bicycles dynamics from the perspective of control can be found in the paper [4] by Astrom, Klein and Lennartsson, where, through models of different complexity, they show a number of interesting dynamics properties and highlight the main difficulties in controlling bicycles. An input-output feedback linearization approach is proposed by Getz and Marsden in [10] in order to design a controller which allows the bicycle to track planar trajectories. Lee and Ham in [11] presented a control strategy for bicycle balancing based on the sliding patch and stuck phenomena of 2nd order nonlinear control system, while Yamakita and Utano in [12] discuss the design of an input-output feedback linearization control for bicycle equipped with a balancer used to guarantee stability also when the speed is zero. A number of different fuzzy control algorithms have been recently proposed in the literature. Guo, Liao and Wei [13] proposed a fuzzy sliding mode controller for bicycles described by a proper nonlinear model, while an adaptive neuro-fuzzy controller for bicycle stability has been presented by Umashankar and Himanshu Dutt Sharma in [14].

In this paper the problem of designing a control system aiming at automatically balancing a riderless bicycle in the upright position is considered. Such a problem is formulated as the design of linear-parameter-varying (LPV) state-feedback controller which guarantees stability of the bicycle when the velocity varies within a given range and its derivative is bounded. The paper is organized as follows. Section II provides a detailed description of the physical plant, i.e. an instrumented bicycle, considered in this work. Then, the mathematical model of the plant is discussed and analyzed in Section III. Further, the control problem is formulated in Section IV where a detailed description of the proposed solution is also presented. Finally, the experimental results obtained testing the design controller on the real bike are reported and discussed in Section V. Concluding remarks can be found in Section VI.

II. Plant description

The plant to be controlled is an instrumented riderless bicycle built during the Master of Science Thesis [15] developed at ABB Corporate Research, Baden, Switzerland in collaboration with the Dipartimento di Automatica e Informatica

V. Cerone and D. Regruto are with Dipartimento di Automatica e Informatica, Politecnico di Torino, Italy email: vito.cerone@polito.it, diego.regruto@polito.it

D. Dzung and D. Andreo are with ABB Switzerland Ltd. email: dacfey.dzung@ch.abb.com, davide.andreo@ch.abb.com

(DAUIN) of Politecnico di Torino, Italy. The prototype of the instrumented bicycle was obtained from a standard city bicycle removing all the unnecessary parts (brakes, chain, crankset and pedals). The bicycle (Figure 1) is equipped with three sensors, one actuator and an industrial processing platform for the implementation of the controller and the signals processing algorithms. The rear wheel is equipped with an encoder in order to measure the bicycle forward speed, while measurements of roll velocity and steering angle are respectively provided by a gyroscope and a potentiometer. Indirect measurements of the roll angle are obtained through numerical integration from the gyroscope output. Since the gyroscope provides a relative measure, the initial condition of the integration is given by a pendulum connected to the bicycle frame through a linear potentiometer. The initial condition of the roll angle is provided by the mean value of the pendulum angle oscillations. The steering angular velocity measurements are indirectly obtained through filtered numerical differentiation of the steering angle. The actuator is a torque driven servo-motor which provides a torque on the steering axis. The maximum value of the torque is ± 1.5Nm. The bicycle is not equipped with active traction on the wheels. The processing platform is a general purpose ABB PEC80 which includes both a computational unit and a data acquisition and communication unit. The control implementation software level of the ABB PEC80 is programmed through Matlab$^{\mathrm{TM}}$/Simulink$^{\mathrm{TM}}$ environment and Matlab Real Time Workshop$^{\mathrm{TM}}$. Thanks to a proprietary toolbox (ABB AC PEC800 Toolbox ver.500) which contains a number of Simulink blocks and functions compatible with the available hardware, a huge number of control structures can be easily implemented. The sample time used for the implementation of the controller presented in this paper is 0.01 s. A detailed description of the ABB PEC80 can be found in [15].

III. Plant modeling

In this paper the bicycle mathematical model proposed by Schwab and co-workers in [7], [9] has been considered for both the analysis of the plant dynamics and the design of the controller. The mechanical model of the bicycle consists of four rigid bodies: the rear frame, the front fork and handlebar assembly, the rear and the front knife-edge wheels. The four bodies are interconnected by revolute hinges and, in the reference configuration, they are all symmetric relatively to the bicycle longitudinal axis. The contact between the stiff non-slipping wheels and the flat level surface is modelled by holonomic constraints in the normal direction and by nonholonomic constraints in the longitudinal and lateral direction. In spite of its relative simplicity, the model adequately describes the main dynamics of the bicycle as proved by the experimental validation performed in [16]. This model considers three degrees of freedom (the roll, the steer, and the forward speed) and has been obtained through linearization of the equations of motion for small perturbation around the so-called constant-speed straight-ahead upright trajectory. The linearized equations of motion are two coupled second-order ordinary differential equations which depends on the forward speed v. The equations, written in matrix form, are the following:

$$\mathbf{M}\ddot{\mathbf{q}} + [v\mathbf{C_1}]\,\dot{\mathbf{q}} + \left[\mathbf{K_0} + v^2\mathbf{K_2}\right]\mathbf{q} = \mathbf{f} \tag{1}$$

with:

$$\mathbf{q}^{\mathrm{T}} = [\phi \quad \delta]\,, \qquad \mathbf{f}^{\mathrm{T}} = [T_\phi \quad T_\delta]$$

where ϕ is the roll angle, δ is the steering angle, v is the bicycle velocity, T_ϕ is a possible exogenous roll torque disturbance and T_δ is the steering torque provided by the actuator. The remaining quantities involved in the equations are the symmetric mass matrix $\mathbf{M}$, the damping matrix $v\mathbf{C_1}$ which is linear in the forward speed v, and the stiffness matrix which is the sum of a constant (symmetric) part, $\mathbf{K_0}$, and a part, $v^2\mathbf{K_2}$, which is quadratic in the forward speed v. These matrices depends on the geometrical parameters of the bicycle (see [7] for details). The obtained linearized equations have been rewritten in state-space form choosing the roll angle ϕ, the steering angle δ and their derivatives, $\dot{\phi}$ and $\dot{\delta}$ respectively, as state variables. The control input $u(t)$ is the torque applied on the handlebar axis, $T_\delta(t)$. The measured output $y(t)$ are all the four state variables. Due to the complexity and non-linear characteristic (with respect to the velocity v) of the equations of motion, the following state-space equations can be straightforwardly derived from (1):

$$\begin{cases} \dot{x}(t) = A(v)x(t) + Bu(t) \\ y(t) = Cx(t) + Du(t) \end{cases} \tag{2}$$

where:

$$x^{\mathrm{T}}(t) = \left[\phi \quad \delta \quad \dot{\phi} \quad \dot{\delta}\right], \quad u(t) = T_\delta, \quad y(t) = \phi \tag{3}$$

and:

$$A = \begin{bmatrix} 0 & 0 & 1 & 0 \\ 0 & 0 & 0 & 1 \\ 13.67 & 0.225 - 1.319v^2 & -0.164v & -0.552v \\ 4.857 & 10.81 - 1.125v^2 & 3.621v & -2.388v \end{bmatrix}$$

$$B = \begin{bmatrix} 0 \\ 0 \\ -0.339 \\ 7.457 \end{bmatrix}, \quad C = \begin{bmatrix} 1 & 0 & 0 & 0 \\ 0 & 1 & 0 & 0 \\ 0 & 0 & 1 & 0 \\ 0 & 0 & 0 & 1 \end{bmatrix}, \quad D = 0 \tag{4}$$

The numerical values of matrices in equation (4) have been derived in [15]. As can be seen from equation (4), matrix A depends on the bicycle forward speed v. Such a dependence qualifies system (2) as a Linear-Parameter-Varying (LPV) model. For each constant value of time-varying parameter v, equation (2) describes an LTI system. The location of the eigenvalues of system (2) for a number of different values of v in the interval $[0, 10]$ m/s is depicted in Figure 2. When the bicycle forward speed v is zero, the system has four real poles at $p_1 = 3.23$, $p_2 = -3.23$, $p_3 = 3.74$ and $p_4 = -3.74$, marked with circles in Figure 2. The first pair of poles corresponds to the so-called pendulum-like poles; the notation is due to the fact that in this condition the bicycle would fall over just like an inverted pendulum. The

remaining pole pair are related to the front fork dynamics. As the velocity increases, the poles p_1 and p_3 meet (at $v \approx 0.5$ m/s) and become complex conjugate. The real part of the complex pole-pair decreases as the velocity increases. Following Sharp ([17]) this mode is called the weave mode, which becomes stable at the critical velocity $v_w \approx 3.4$ m/s. The pole p_2 remains real and moves toward the right half plane with increasing velocity. It becomes unstable at the velocity $v_c \approx 4.1$ m/s. The pole p_4 moves to the left as velocity increases. For large velocity v, the pole p_2 approaches zero. The values of v_w and v_c strongly depend on the value of the bicycle trail (see [4] for details). From the above analysis it is clear that the task of controlling a riderless bicycle is a challenging problem, since the plant dynamics strongly depends on the bicycle forward speed.

IV. Control problem formulation and proposed solution

The problem we are dealing with in this paper is the design of a control system in order to automatically balance a riderless bicycle in the upright position. Such a problem can be formulated as the design of a feedback controller able to guarantee stability of the LPV system described by the equations (2) when the velocity v is allowed to vary in the interval $[0, \gamma]$ and its derivative $\dot{v}$ satisfies the constraint $|\dot{v}| \leq \rho$ where γ and ρ are known constants. As is well known stability of all the frozen LTI systems obtained for each fixed values of v is not a sufficient condition for the stability of the LPV system. As stated in Section II, the bicycle under consideration is not equipped with a wheels active traction system, thus, in the experimental tests, a human operator makes the bicycle run by pushing it for a few seconds. According to such experimental conditions, reasonable values for γ and ρ are respectively $\gamma = 5$ m/s and $\rho = 0.5$ m/s^2. Since all the state variables of systems (2) are available for measurements, a static state-feedback control structure has been chosen. The dynamics of the system to be controlled depends on the time-varying parameter v and on-line measurements of such a parameter are available (see Section II), thus we look for an LPV controller of the form $u = K(v)x = [k_\phi(v)\ k_\delta(v)\ k_{\dot{\phi}}(v)\ k_{\dot{\delta}}(v)]x^{\mathrm{T}}$ which on the basis of the measurements of v and $x(t)$ provides the control input $u(t)$ that guarantees stability of the closed loop LPV systems when $\in [0, \gamma]$ and $|\dot{v}| \leq \rho$. The following proposition, derived from the application of Theorem 14 of paper [18] to the problem considered in this work, provides the basis for the design of such a controller.

Proposition 1 [18] *The closed loop system described by equation*

$$\dot{x} = A_{cl}(v)x, \qquad A_{cl}(v) = A(v) + BK(v) \tag{5}$$

is exponentially stable for all the trajectory of the velocity v satisfying $v \in [0, \gamma]$ and $|\dot{v}(t)| \leq \rho$ if there exists a matrix $X(v) = X^{\mathrm{T}}(v) > 0$ such that

$$X(v)A_{cl}(v) + A_{cl}^{\mathrm{T}}(v)X(v) + \dot{v}\frac{dX(v)}{dv} < 0 \tag{6}$$

for all $v \in [0, \gamma]$ and $|\dot{v}| \leq \rho$.

Proposition 1 clearly states that the problem of designing a feedback controller able to guarantee exponential stability of the LPV system described by the equations (2) can be solved by performing a numerical search for a pair of parameter dependent matrices $X(v)$ and $K(v)$ which satisfy the matrix inequality (6). Unfortunately, since inequality (6) is a nonconvex constraint in the variables $X(v)$ and $K(v)$, a direct numerical search leads to a nonconvex optimization problem. However, by means of some simple manipulations (see [18] for details), it can be shown that the existence of a pair of matrices $X(v)$ and $K(v)$ satisfying the nonconvex constraint (6) is equivalent to the existence of the matrices

$$Y(v) = X^{-1}(v) \quad \text{and} \quad \overline{K}(v) = K(v)X^{-1}(v) \tag{7}$$

which satisfy the following linear matrix inequality (LMI):

$$A(v)Y(v) + B\overline{K}(v) + Y(v)A^{\mathrm{T}}(v) + \overline{K}^{\,\mathrm{T}}(v)B^{\mathrm{T}} - \dot{v}\frac{dY(v)}{dv} < 0 \tag{8}$$

As is well known, computing solutions to LMIs leads to a special kind of convex optimization problem for which efficient numerical solutions are available (see, e.g., [19]).

Due to the dependence on the parameter v, equation (8) actually represents an infinite family of LMIs. As properly discussed in [18], a possible approach to reduce the problem to the solution of a finite set of LMIs is the parameter discretization. More precisely, by dividing the interval $[0, \gamma]$ into N subintervals of width h and exploiting a forward difference approximation for the derivative, the constraint (8) is approximately converted to the following finite collection of LMIs:

$$\begin{aligned} &A(jh)Y(jh) + B\overline{K}(jh) + Y(jh)A^{\mathrm{T}}(jh) + \overline{K}^{\,\mathrm{T}}(jh)B^{\mathrm{T}} + \\ &\pm\rho\frac{Y(jh+h) - Y(jh)}{h} < 0, \quad j = 0, ..., N-1 \end{aligned} \tag{9}$$

The discretization has been performed in this work choosing $N = 100$ and $h = 0.05$ m/s.

In order to bound the damping ζ and the natural frequency ω_n of the eigenvalues of the matrix $A_{cl}(v)$ for each fixed value of $v = jh$ obtained from the discretization of the interval $[0, \gamma]$, the following two sets of constraints are added to the design problem:

$$\begin{bmatrix} -rY(jh) & A(jh)Y(jh) + B(jh)\overline{K}(jh) \\ Y(jh)A(jh)^{\mathrm{T}} + \overline{K}^{\,\mathrm{T}}(jh)B^{\mathrm{T}} & -rY(jh) \end{bmatrix} < 0, \quad \text{for } j = 0, ..., N-1 \tag{10}$$

and

$$\begin{bmatrix} \sin\theta(A(jh)Y(jh) + B\overline{K}(jh) + Y(jh)A(jh)^{\mathrm{T}} + \overline{K}^{\,\mathrm{T}}(jh)B^{\mathrm{T}}) \\ \cos\theta(Y(jh)A(jh)^{\mathrm{T}} - \overline{K}^{\,\mathrm{T}}(jh)B^{\mathrm{T}} - A(jh)Y(jh) - B\overline{K}(jh)) \\ \cos\theta(A(jh)Y(jh) + B\overline{K}(jh) - Y(jh)A(jh)^{\mathrm{T}} - \overline{K}^{\,\mathrm{T}}(jh)B^{\mathrm{T}}) \\ \sin\theta(A(jh)Y(jh) + B\overline{K}(jh) + Y(jh)A(jh)^{\mathrm{T}} + \overline{K}^{\,\mathrm{T}}(jh)B^{\mathrm{T}}) \end{bmatrix} < 0, \quad \text{for } j = 0, ..., N-1 \tag{11}$$

Equations (10) and (11) are LMIs in the variables $Y(jh)$ and $\overline{K}(jh)$ which guarantee a minimum damping ratio $\zeta = \cos\theta$ and a maximum natural frequency $\omega_n = r\sin\theta$ for the eigenvalues of the closed loop systems computed at each fixed value of v (see paper [20] and the references therein for a detailed description on how to describe constraints on eigenvalues location in terms of LMIs). In this work the values $\zeta = 0.6$ and $\omega_n = 20$ rad/s have been considered which correspond to the values $r \approx 25$ rad/s and $\theta \approx 0.93$ rad. The value $\zeta = 0.6$ has been chosen in order to avoid significantly under-damped oscillation in the response; the value of ω_n has been chosen on the basis of the simulation performed exploiting the mathematical model of the plant which revealed that a value greater than 20 rad/s leads to saturation of the actuator. The set of LMIs described by equations (9), (10) and (11) have been solved using the LMI toolbox of MatLab$^{\mathrm{TM}}$. The obtained solution is a collection of discretized variables $Y(jh)$ and $\overline{K}(jh)$. A continuous solution $Y(v)$, $\overline{K}(v)$ has been formed by interpolation. Finally, the controller gains $K(v)$ have been obtained from (7) as $K(v) = \overline{K}(v)Y(v)^{-1}$. The location of the closed loop eigenvalues when v ranges in $[0, 5]$ m/s is depicted in Fig. 3.

Remark – An alternative approach to reduce problem (8) to the solution of a finite set of LMIs is to impose a fixed structure on the search variables $Y(v) = X^{-1}(v)$ and $\overline{K}(v)$ avoiding parameter discretization. However, in that case, some conservatism is introduced in the problem (see, e.g., [18] for details). For such a reason, in this work we have chosen to exploit the gridding approach. Besides, we would like to remark that the bicycle dynamics depends on a single parameter and, thus, a fine discretization can be performed.

V. Experimental results and discussion

In this section we report the experimental results obtained testing the controlled systems. As stated in Section II, the bicycle under consideration is not equipped with a wheels active traction system; thus, in all the experimental tests, a human operator pushes the bicycle for a few seconds, then the bicycle is released. All the experimental data reported in the figures of this section have been collected from the time the human operator releases the bicycle. Since the tests were performed in a room of limited dimension, the maximum bicycle velocity considered was about 2.1 m/s. However, we would like to remark that the control of a riderless bicycle is more challenging at such low velocities, since, as stated in Section III, the system is open loop unstable for values of velocity v less that 3.4 m/s. Three different experimental tests, described below, have been performed.

A. Uncontrolled bicycle

In the first test the bicycle ran with the control system switched off. Such a test was performed to show that the open-loop riderless bicycle is unstable when the velocity v is less than 3.4 m/s. The bicycle has been pushed to a velocity of about 3m/s and then released. The evolution of the roll angle $\phi(t)$ is shown in Figure 4. As expected, after few seconds $\phi(t)$ rapidly increases reaching a value of about 20 degrees just before falling down.

B. Controlled bicycle, $1m/s \leq v \leq 1.7m/s$

In this test the bicycle was pushed by the human operator until the velocity reached the value of 1.7 m/s; then it was released. The test stopped when the bicycle reached the end of the room. The final velocity was 1 m/s. The evolution of the roll angle $\phi(t)$ is shown in Figure 5, from which it can be seen that the designed LPV control system effectively balances the riderless bicycle in the upright position. As a matter of fact, after about 10 s, the amplitude of the bicycle roll angle $\phi(t)$ is driven to a value of about 0.1 degrees starting from the initial condition $\phi(0) \approx -2.25$ degrees. The steering torque T_δ applied on the handlebar axis to control the bicycle is reported in Figure 6. Figure 7 reports the velocity of the bike, while Figure 8 shows the values of the state-feedback gains $K(v)$.

C. Controlled bicycle, 1.7m/s$\leq v \leq$ 2.1m/s and external impulsive roll torque disturbance

In this test the bicycle was pushed by the human operator until the velocity reached the value of 2.1 m/s, then it was released. The test stopped when the bicycle reached the end of the room. The final velocity was 1.7 m/s. In order to evaluate the robustness of the designed control system against exogenous disturbances (like for example a side wind gust), the human operator slapped the rear frame of the bicycle. Such a "slap" can be modeled as an impulsive roll torque disturbance of about 26 Nm (see [15] for details on the approximate characterization of such a disturbance). The lateral disturbance was applied just after the time the bicycle was released. The experimental data reported in the figures of this section have been collected from the time the roll torque disturbance has been applied to the bicycle. The evolution of the roll angle $\phi(t)$ is shown in Figure 9, from which it can be seen that the designed LPV control system effectively balances the riderless bicycle in the upright position, also in the presence of the roll torque disturbance. As a consequence of the "slap", the bike roll angle reaches a maximum value of about -2.75 degrees ($t \approx 0.6$s), then it is rapidly attenuated by the control system to a value less than 0.75 degrees ($t \approx 6.5$s). The steering torque T_δ applied on the handlebar axis to control the bicycle is reported in Figure 10. Figure 11 reports the velocity of the bike, while Figure 12 shows the values of the state-feedback gains $K(v)$.

VI. Conclusions

In this paper the problem of designing a control system aiming at automatically balancing a riderless bicycle in the upright position is considered. Such a problem is formulated as the design of linear-parameter-varying (LPV) state-feedback controller able to guarantee stability of the bicycle when the velocity is allowed to vary in a known interval and its derivative is bounded. The controller has been designed solving an LMI optimization problem. The designed control system has been implemented on a real riderless bicycle

equipped with suitable sensors and actuators, and exploiting the processing platform ABB PEC80. The obtained experimental results showed the effectiveness of the proposed approach.

ACKNOWLEDGEMENTS

We thank Mats Larsson of ABB Corporate Research for his crucial contributions to the bicycle modeling, and Paul Rudolf for the support in setting up the hardware.

REFERENCES

[1] W. J. M. Rankine, "On the dynamical principles of the motion of velocipedes," *Engineer*, vol. 28, pp. 79, 129, 153, 175, 1869.
[2] F. J. W. Whipple, "The stability of the motion of a bicycle," *The Quarterly Journal of Pure and Applied Mathematics*, vol. 30, no. 120, pp. 312–348, 1899.
[3] E. Carvallo, "Theorie du mouvement du monocycle et de la bicyclette," *Journal de l'Ecole Polytechnique*, vol. 5, pp. 119–188, 1900.
[4] K. J. Astrom, R. E. Klein, and A. Lennartsson, "Bicycle dynamics and control," *IEEE Control Systems Magazine*, vol. 25, no. 4, pp. 26–47, 2005.
[5] D. J. N. Limebeer and R. S. Sharp, "Bicycles, motorcycles and models," *IEEE Control Systems Magazine*, vol. 6, no. 5, pp. 34–61, 2006.
[6] R. D. Roland, "Computer simulation of bicycle dynamics," *Mechanics and Sport*, vol. AMD-4, no. New York: ASME, pp. 35–83, 1973.
[7] A. L. Schwab, J. P. Meijaard, and J. M. Papadopoulos, "Benchmark results on the linearized equations of motion of an uncontrolled bicycle," in *Proceedings of the The Second Asian Conference on Multibody Dynamics 2004, Seoul, Korea*, 2004.
[8] ——, "A multibody dynamics benchmark on the equations of motion of an uncontrolled bicycle," in *Proceedings of the Fifth EUROMECH Nonlinear Dynamics Conference, August 7-12, 2005, Eindhoven University of Technology, The Netherlands*, 2005, pp. 511–521.
[9] J. P. Meijaard, J. M. Papadopoulos, A. Ruina, and A. L. Schwab, "Linearized dynamics equations for the balance and steer of a bicycle: a benchmark and review," *Proceedings of the Royal Society*, vol. A463, pp. 1955–1982, 2007.
[10] N. H. Getz and J. E. Marsden, "Control for an autonomous bicycle," in *IEEE International Conference on Robotics and Automation*, 1995, pp. 1397–1402.
[11] S. Lee and W. Ham, "Self stabilizing strategy in tracking control of an unmanned electric bicycle with mass balance," in *Proceedings of the IEEE Conference on Intelligent Robots Systems, Lausanne, Switzerland*, 2002, pp. 220–220.
[12] M. Yamakita and A. Utano, "Automatic control of bicycles with a balancer," in *Proceedings of IEEE/ASME Conference on Advanced Intelligent Mechatronics, Monterey, California, USA*, 2005, pp. 1245–1250.
[13] L. Guo, Q. Liao, and S. Wei, "Design of fuzzy sliding mode controller for bicycle robot nonlinear system," in *Proceedings of IEEE Conference on Robotics and Biomimetics, Kunming, China*, 2006, pp. 176–180.
[14] N. Umashankar and H. D. Sharma, "Adaptive neuro - fuzzy controller for stabilizing autonomous bicycles," in *Proceedings of IEEE Conference on Robotics and Biomimetics, Kunming, China*, 2006, pp. 1652–1657.
[15] D. Andreo, *Feedback Control Design and Hardware Setup for a Riderless Bike*. MSc Thesis, Politecnico di Torino, Italy, 2008.
[16] J. D. G. Kooijman, *Experimental Validation of a Model for the Motion of an Uncontrolled Bicycle*. MSc Thesis, Delft University of Technology, The Netherlands, 2006.
[17] R. S. Sharp, "The stability and control of motorcycles," *Journal of Mechanical Engineering*, vol. 13, no. 5, pp. 316–329, 1971.
[18] W. J. Rugh and J. S. Shamma, "Research on gain scheduling," *Automatica*, vol. 36, no. 10, pp. 1401–1425, 2000.
[19] S. Boyd, L. E. Ghaoui, E. Feron, and V. Balakrishnan, *Linear matrix inequalities in system and control theory*. SIAM, 1994.
[20] M. Chilali and P. Gahinet, "H_∞ with pole placement constraints: an LMI approach," *IEEE Transaction on Automatic Control*, vol. 41, no. 3, pp. 358–367, 1996.

Fig. 1. The instrumented bicycle used in this work

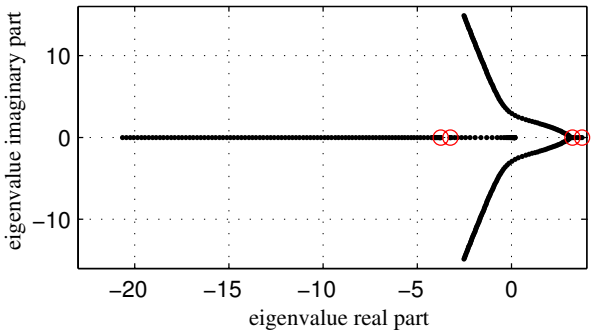

Fig. 2. Poles trajectory for the uncontrolled bike (speed range (0,10)m/s). The poles marked with circles correspond to $v = 0m/s$.

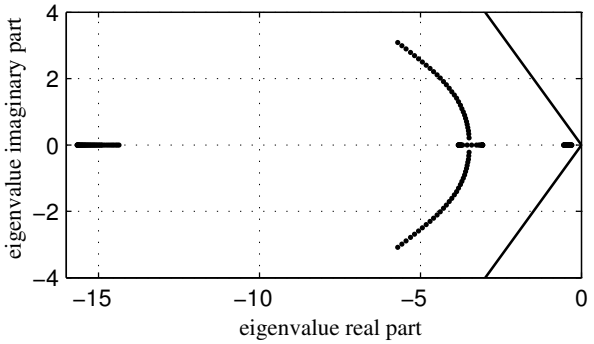

Fig. 3. Root locus for the controlled bike eigenvalues (speed range $[0, 5]$ m/s) and damping constraints (straight thin lines)

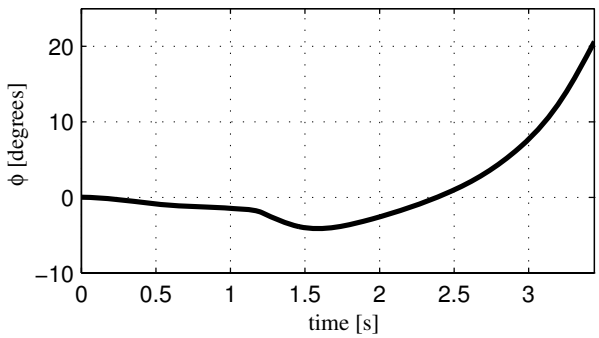

Fig. 4. Uncontrolled bicycle: roll angle

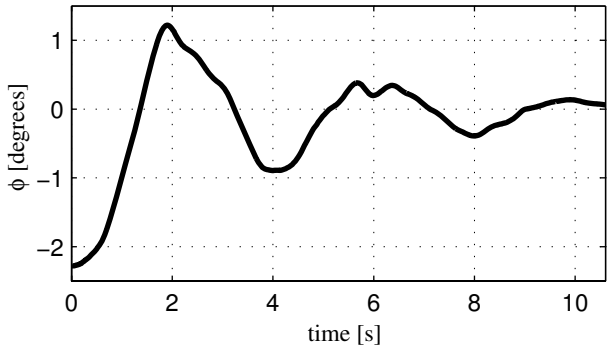

Fig. 5. Controlled bicycle without external disturbance: roll angle

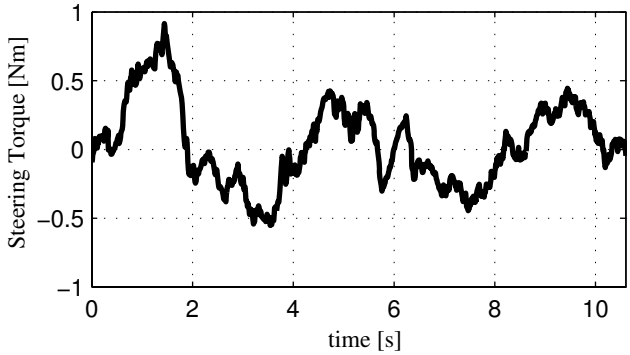

Fig. 6. Controlled bicycle without external disturbance: steering torque

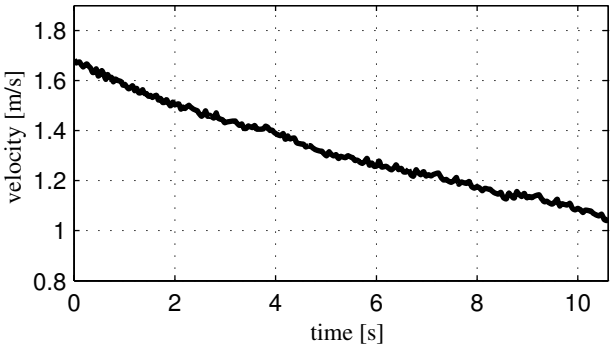

Fig. 7. Controlled bicycle without external disturbance: velocity

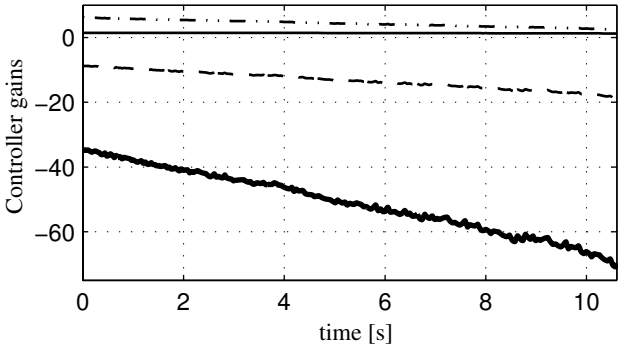

Fig. 8. Controlled bicycle without external disturbance: controller gains k_ϕ (thick), k_δ (dash-dot), $k_{\dot{\phi}}$ (thin), $k_{\dot{\delta}}$ (dashed)

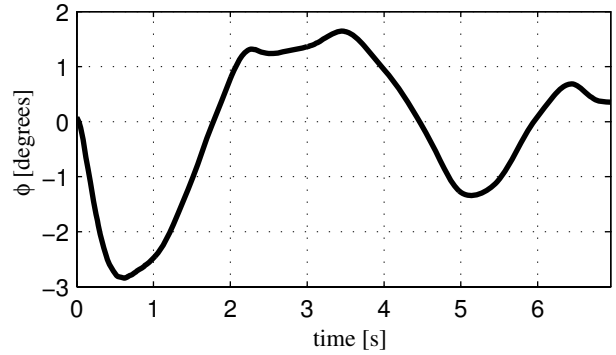

Fig. 9. Controlled bicycle in presence of an external impulsive roll torque disturbance: roll angle

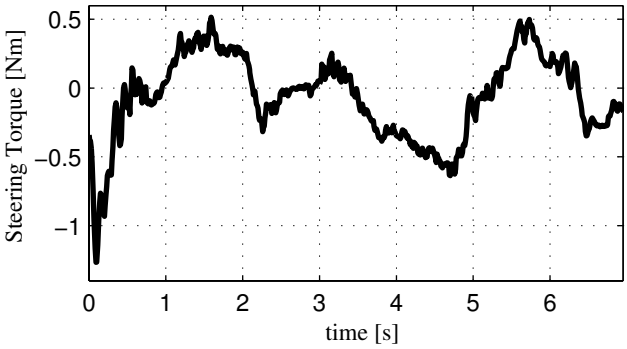

Fig. 10. Controlled bicycle in presence of an external impulsive roll torque disturbance: steering torque

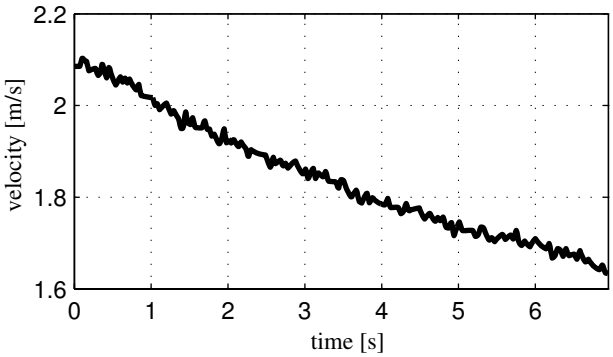

Fig. 11. Controlled bicycle in presence of an external impulsive roll torque disturbance: velocity

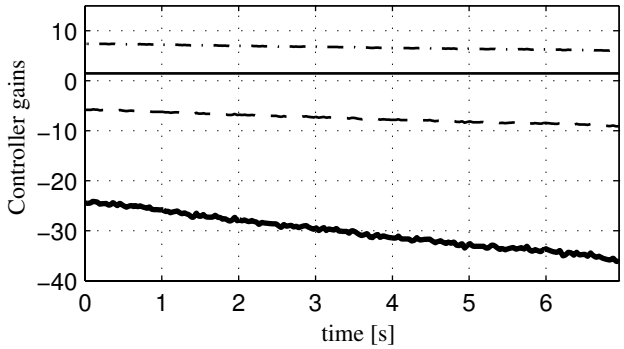

Fig. 12. Controlled bicycle in presence of an external impulsive roll torque disturbance: controller gains k_ϕ (thick), k_δ (dash-dot), $k_{\dot{\phi}}$ (thin), $k_{\dot{\delta}}$ (dashed)